



**Modeling Ultrasound-Induced Molecular Weight Decrease of  
Polymers with Multiple Scissile Azo-Mechanophores**

Journal:	<i>Polymer Chemistry</i>
Manuscript ID	PY-ART-03-2021-000420.R1
Article Type:	Paper
Date Submitted by the Author:	29-May-2021
Complete List of Authors:	Ayer, Mathieu; Adolphe Merkle Institute, University of Fribourg, Polymer Chemistry and Materials Verde-Sesto, Ester ; University of the Basque Country UPV/EHU, Materials Physics Center Liu, Cheyenne ; University of Southern Mississippi, School of Polymer Science and Engineering Weder, Christoph; Adolphe Merkle Institute, University of Fribourg, Polymer Chemistry and Materials Lattuada, Marco; Universite de Fribourg, Adolphe Merkle Institute; Simon, Yoan; University of Southern Mississippi, School of Polymer Science and Engineering;



Journal Name

ARTICLE

## Modeling Ultrasound-Induced Molecular Weight Decrease of Polymers with Multiple Scissile Azo-Mechanophores

Mathieu A. Ayer,<sup>a</sup> Ester Verde-Sesto,<sup>a,b</sup> Cheyenne H. Liu,<sup>c</sup> Christoph Weder,<sup>a</sup> Marco Lattuada<sup>\*a,d</sup> and Yoan C. Simon<sup>\*a,c</sup>

Received 00th January 20xx,  
Accepted 00th January 20xx

DOI: 10.1039/x0xx00000x

[www.rsc.org/](http://www.rsc.org/)

The azo moiety is receiving increasing attention as a stimuli-responsive trigger. Herein, we present an investigation of the mechanoresponsive behavior of a series of polyurethanes containing multiple randomly distributed azo motifs as scissile mechanophores, *i.e.*, an entity that is preferentially cleaved upon application of a mechanical force. We made a systematic comparison of the ultrasound-induced cleavage of azo-containing polymers of different molecular weights and with varying azo content. We developed a mathematical model to describe the scission kinetics and the analysis of the rate constants showed that site-specific cleavage at the azo position was favored over random bond scission events. The proposed mathematical model appears to be a broadly useful method to characterize the ultrasound-induced molecular weight decrease of polymers containing multiple scissile mechanophores.

### Introduction

Mechanochemical reactions allow for the transduction of mechanical forces into chemical reactions, which one can harness to impart polymers with mechanoresponsive behaviors.<sup>1</sup> The number of compelling macromolecular materials that display tailored, mechanically induced responses in the solid state is rapidly increasing; examples include polymers that display changes in color<sup>2</sup> or emission properties,<sup>3,4</sup> actuation,<sup>5</sup> generation of acids<sup>6,7</sup> or bases,<sup>8</sup> or release of small molecules.<sup>9,10</sup> All of these effects make polymer mechanochemistry very attractive for use in applications such as sensing,<sup>11,12</sup> mechanomorphing,<sup>13</sup> catalysis,<sup>14</sup> healable materials<sup>15</sup> or even drug release.<sup>16</sup> These remarkable properties and functions are achieved through the incorporation of specific, mechanically activable motifs within the polymer chain, referred to as mechanophores, and serve to transduce mechanical forces into often very specific chemical reactions. Emergent research in mechanochemistry at interfaces<sup>17,18</sup> as well as in complex polymeric architectures, including single-chain nanoparticles,<sup>19</sup> rotaxanes,<sup>20,21</sup> catenanes,<sup>22,23</sup> macrocycles,<sup>24</sup> and micelles,<sup>25</sup> demonstrates the broad applicability of mechanochemical activation in polymers.

Aside from solid-state experiments, the utilization of ultrasound to generate elongational forces and elicit the mechanochemical cleavage of macromolecules in solution is widespread.<sup>26</sup> New mechanophores are often probed by sonochemical studies in solution. Conversely, the quest for the discovery of new mechanophores inducing unusual functions has also furthered the understanding of ultrasound-induced polymer mechanochemistry.<sup>27</sup> A great deal of work has focused on understanding the ultrasonic cleavage mechanisms of polymers with and without a single, chain-centered mechanophore.<sup>28-37</sup> For instance, early work by Berkowski *et al.* investigated the rate of the ultrasonic cleavage of different azo-functionalized poly(ethylene glycol)s.<sup>38</sup> Two studies have focused on the cleavage of polymers containing respectively a centered palladium carbene complex and a centered spiropyran to obtain insight into the parameters influencing the ultrasound-induced response, *i.e.*, the activation efficiency at low forces and the degree of polymerization.<sup>8,27</sup> Ultimately, single mechanophore systems are limited in responsiveness as a direct result of competitive, non-selective scission events and corresponding incomplete mechanophore activation.

Naturally, multi-mechanophore systems offer an attractive solution towards maximizing mechanochemical response and have been actively pursued from the onset.<sup>39-43</sup> Although multi-mechanophore systems have been reviewed recently,<sup>44</sup> detailed sonochemical kinetic studies and fundamental understanding of such systems, either scissile or non-scissile, are sparse. Many of the early studies emphasized polymers containing non-scissile ring-opening and/or regularly spaced mechanophores.<sup>13,39-43,45-49</sup> Importantly, recent work by Stevenson *et al.* has shown that a centered, scissile bismechanophore system in close proximity did not exhibit faster scission kinetics than a single mechanophore system despite variation in adduct orientation and tether location. This

<sup>a</sup> Adolphe Merkle Institute, University of Fribourg, Chemin des Verdiers 4, 1700 Fribourg, Switzerland.

<sup>b</sup> Centro de Física de Materiales (CSIC, UPV/EHU) and Materials Physics Center MPC, Paseo Manuel de Lardizabal 5, E-20018 San Sebastián, Spain

<sup>c</sup> School of Polymer Science and Engineering, The University of Southern Mississippi, 118 College Dr., Hattiesburg MS 39406, USA. Email: yoan.simon@usm.edu

<sup>d</sup> Department of Chemistry, University of Fribourg, Chemin du Musée 9, 1700-Fribourg, Switzerland. Email: marco.lattuada@unifr.ch

Electronic Supplementary Information (ESI) available: FT-IR, NMR, SEC analyses and details about the mathematical modeling and light irradiation experiments. See DOI: 10.1039/x0xx00000x

result suggests that multi-mechanophore systems are nuanced in both number and spacing of individual mechanically active moieties in order to elicit a useful response.<sup>50</sup> Lee *et al.* published a compelling study on a copolymer system containing one of three different mechanophores with weak scissile mechanophores and the non-scissile *gem*-dichlorocyclopropane (*gDCC*) motif in the backbone. A comparative analysis that exploited the non-scissile ring-opening process of the *gDCC* moieties as reference revealed that azobisdialkyl nitrile (azo) motifs were weaker and dissociated more easily than thioether and benzylphenyl ether linkages.<sup>51</sup>

Few examples in the literature thoroughly describe chain scission kinetics of polymers that contain multiple, scissile mechanophores along the backbone.<sup>52–54</sup> Di Giannantonio *et al.* have modeled the kinetics of poly(methyl acrylate) and poly(urethane) systems containing a single or multiple ferrocene mechanophores. This strategy yielded greater sensitivity in the detection of ferrocene dissociation, and two distinct rate constants associated with non-selective chain scission and ferrocene dissociation were identified.<sup>52</sup> Work by Sha *et al.* extended this study to related main-chain ruthenocene mechanophores, where a multi mechanophore approach was taken to probe ruthenocene mechanoreactivity.<sup>53,55</sup>

Building upon our previous work on the synthesis and investigation of thermo- and photo-responsive properties of azo-containing polymers,<sup>56,57</sup> we report herein a detailed kinetic study of the ultrasound-induced chain scission of various polyurethanes with randomly positioned azo motifs. Azo motifs have garnered renewed interest for their multi-stimuli responsive characteristics.<sup>58–61</sup> A new kinetic model was applied for the analysis of size-exclusion chromatography (SEC) data acquired after ultrasonication experiments with reference polyurethanes (**ref-PU**s, *i.e.*, without mechanophore) and polyurethanes containing several mechanophores (**azo-PU**s). The average number of azo motifs in the latter was controlled *via* the monomer composition employed for the step-growth polymerizations used to prepare these materials. The influence of the number of azo motifs per chain and the molecular weight of the polyurethanes on the ultrasound-induced cleavage was investigated. Expectedly, two competitive scission events, site-specific (azo motifs) *vs.* random bond cleavages, were observed. The rate constant of random bond scission proved to be significantly slower than that of the site-specific cleavage.

## Experimental section

### Materials

Inhibitor-free anhydrous tetrahydrofuran (THF) (Sigma-Aldrich) was used as solvent for the polymer syntheses. Poly(tetrahydrofuran) (PTHF, number-average molecular weight,  $M_n = 2,000$  g/mol) was dried *in vacuo* at 100 °C for 1 h before use. 4,4'-methylenebis(phenyl isocyanate) (MDI) and 1,4-butanediol (BDO) were distilled under vacuum and stored over molecular sieves at 5 °C. 2,2'-Azobis[2-methyl-*N*-(2-hydroxyethyl)propionamide] (**1**) was kindly offered by Wako

Pure Chemicals Industries (VA-086) and was dried *in vacuo* at room temperature (rt) overnight immediately before use. All other reagents were obtained, unless otherwise mentioned, from Sigma-Aldrich and used without further purification.

### Instrumentation

<sup>1</sup>H NMR and <sup>13</sup>C NMR spectra were measured on a Bruker Avance III HD spectrometer at 400 MHz (<sup>1</sup>H) and 100 MHz (<sup>13</sup>C), respectively. The chemical shifts ( $\delta$ ) are indicated in parts per million (ppm) relative to tetramethylsilane, although referencing relied on the residual solvent protons. Size-exclusion chromatography (SEC) analyses were performed on an Agilent Technologies 1200 system equipped with a Wyatt Optilab rEX differential refractive index (dRI) and a Wyatt miniDAWN TREOS multi-angle laser light scattering (MALLS) detector. The column system consisted of an Agilent 5  $\mu$ m MIXED-C guard column and an Agilent PLgel 5  $\mu$ m Mixed-D (200–400,000 g/mol) column set. The measurements were carried out in THF at a flow rate of 1 mL/min. The mass-average molecular weight ( $M_w$ ) and  $M_n$  values were determined comparatively to poly(styrene) (PS) standards. The dispersity ( $\mathcal{D}$ ) was calculated by the ratio  $M_w/M_n$ . Elemental analysis (EA) was accomplished on a CE Instruments EA 1110 with flash combustion and GC separation. Fourier transform infrared (FT-IR) spectra were measured on a PerkinElmer Spectrum 65 spectrometer having an attenuated total reflection (ATR) system.

### Sonication experiments

The experiments were performed using a Branson Model 450 digital sonifier equipped with a 13 mm tip. A VWR MX07R-20 cooling/heating bath containing a mixture of water/ethylene glycol (1:1 v/v) was employed to maintain the solution temperature at 0 °C. The polymers were dissolved in THF (Romil-SpS™, Super Purity Solvent grade) at a concentration of 0.75 mg/mL. A volume of 20 mL was introduced into a Suslick cell that was then placed into the thermostatic bath. The solutions were purged with argon during 15 min prior to sonication. A pulsed sonication of 0.5 s at a power density of 10.4 W/cm<sup>2</sup> intercalated with pauses of 1.0 s was performed. Aliquots (400  $\mu$ L) were taken with syringes at regular time intervals and introduced into 1 mL vials. For SEC measurements, the solvent was evaporated *in vacuo* at rt and the polymer residues were redissolved in 300  $\mu$ L of THF to create solutions with a concentration of 1 mg/mL.

### UV light irradiation procedure.

Further degradation of the residual azo moieties was provoked by irradiating previously sonicated polymer solutions (1 mL in a 4 mL vial, 0.75 mg/mL) with UV light under stirring using a Hönle Bluepoint 4 Ecocure UV lamp. A 320–390 nm filter was mounted and the power density was kept at *ca.* 600 mW/cm<sup>2</sup> (*i.e.*, the distance between the optical fiber and the center of the vial was of 15 mm). SEC measurements were realized after irradiation. The solvent was subsequently evaporated *in vacuo* at rt and the polymer residues were re-dissolved in SEC quality THF (0.5 mL) to afford a concentration of 1.5 mg/mL.

### Syntheses of azo-PU1 to 4, ref-PU1 and ref-PU2.

These polymers were synthesized using a protocol previously reported by our group.<sup>56</sup> The number of azo motifs per chain was varied from *ca.* 9 (**azo-PU1**) to 0 (**ref-PU**s).

#### azo-PU1 (containing *ca.* 9 azo motifs per chain)

PTHF (2.009 g, 1.005 mmol), **1** (0.072 g, 0.251 mmol), BDO (0.174 g, 1.930 mmol), MDI (0.956 g, 3.822 mmol, NCO/OH molar ratio *ca.* 1.20:1), dibutyltin dilaurate (DBTDL, 3 drops), and THF (30 mL). **azo-PU1** was obtained as a white fibrous, rubbery solid (2.729 g, 85%).  $M_n(\text{SEC}) = 119,000$  g/mol;  $\bar{D} = 1.62$ .  $^1\text{H NMR}$  (THF- $d_8$ , 400 MHz):  $\delta$  = MDI residue: 8.57 (s, 2H, NH), 8.54 (s, 2H, NH), 7.36 (d, 4H, ArH), 7.03 (d, 4H, ArH), 3.82 (s, 2H, CH<sub>2</sub>-Ar); PTHF residue: 4.09 (t, 4H, CH<sub>2</sub>-OOC), 3.37 (s, 108H, CH<sub>2</sub>-O), 1.69 (s, 4H, CH<sub>2</sub>), 1.58 (s, 108H, CH<sub>2</sub>); BDO residue: 4.12 (d, 4H, CH<sub>2</sub>-O), 1.73 (4H, CH<sub>2</sub> obstructed); **1** residue: 8.69 (s, 2H, NH), 7.30 (s, 2H, NH), 4.16 (t, 4H, CH<sub>2</sub>-OOC), 3.48 (q, 4H, CH<sub>2</sub>-NH), 1.33 (s, 12H, CH<sub>3</sub>); end groups: 7.88 (s, 2H, NH<sub>2</sub>), 7.88 (s, 2H, NH<sub>2</sub>), 6.81 (d, 2H, ArH), 6.46 (d, 2H, ArH).

#### azo-PU2 (containing *ca.* 3 azo motifs per chain):

PTHF (2.008 g, 1.004 mmol), **1** (0.034 g, 0.119 mmol), BDO (0.153 g, 1.693 mmol), MDI (0.776 g, 3.102 mmol, NCO/OH molar ratio *ca.* 1.10:1), DBTDL (3 drops), and THF (30 mL). **azo-PU2** was obtained as a white fibrous, rubbery solid (2.750 g, 93%).  $M_n(\text{SEC}) = 70,900$  g/mol;  $\bar{D} = 1.59$ .  $^1\text{H NMR}$  (THF- $d_8$ , 400 MHz):  $\delta$  = MDI residue: 8.57 (s, 2H, NH), 8.54 (s, 2H, NH), 7.36 (d, 4H, ArH), 7.03 (d, 4H, ArH), 3.82 (s, 2H, CH<sub>2</sub>-Ar); PTHF residue: 4.09 (t, 4H, CH<sub>2</sub>-OOC), 3.36 (s, 108H, CH<sub>2</sub>-O), 1.69 (s, 4H, CH<sub>2</sub>), 1.58 (s, 108H, CH<sub>2</sub>); BDO residue: 4.12 (d, 4H, CH<sub>2</sub>-O), 1.73 (4H, CH<sub>2</sub> obstructed); **1** residue: 8.68 (s, 2H, NH), 7.30 (s, 2H, NH), 4.16 (t, 4H, CH<sub>2</sub>-OOC), 3.48 (q, 4H, CH<sub>2</sub>-NH), 1.33 (s, 12H, CH<sub>3</sub>); end groups: 7.65 (s, 2H, NH<sub>2</sub>), 6.81 (d, 2H, ArH), 6.46 (d, 2H, ArH).

#### azo-PU3 (containing *ca.* 9 azo motifs per chain)

PTHF (4.214 g, 2.107 mmol), **1** (0.346 g, 1.200 mmol), BDO (0.356 g, 3.950 mmol), MDI (1.991 g, 7.957 mmol, NCO/OH molar ratio *ca.* 1.10:1), DBTDL (3 drops), and THF (30 mL). **azo-PU3** was obtained as a white fibrous, rubbery solid (5.823 g, 84%).  $M_n(\text{SEC}) = 51,300$  g/mol;  $\bar{D} = 1.50$ .  $^1\text{H NMR}$  (THF- $d_8$ , 400 MHz):  $\delta$  = MDI residue: 8.57 (s, 2H, NH), 8.55 (s, 2H, NH), 7.36 (d, 4H, ArH), 7.04 (d, 4H, ArH), 3.82 (s, 2H, CH<sub>2</sub>-Ar); PTHF residue: 4.10 (t, 4H, CH<sub>2</sub>-OOC), 3.37 (s, 108H, CH<sub>2</sub>-O), 1.69 (s, 4H, CH<sub>2</sub>), 1.59 (s, 108H, CH<sub>2</sub>); BDO residue: 4.13 (d, 4H, CH<sub>2</sub>-O), 1.73 (4H, CH<sub>2</sub> obstructed); **1** residue: 8.69 (s, 2H, NH), 7.30 (s, 2H, NH), 4.16 (t, 4H, CH<sub>2</sub>-OOC), 3.48 (q, 4H, CH<sub>2</sub>-NH), 1.33 (s, 12H, CH<sub>3</sub>); end groups: 6.82 (d, 2H, ArH), 6.47 (d, 2H, ArH), 4.65 (s, 2H, NH<sub>2</sub>).

#### azo-PU4 (containing *ca.* 0.5 azo motifs per chain)

PTHF (2.033 g, 1.016 mmol), **1** (0.005 g, 0.016 mmol), BDO (0.153 g, 1.693 mmol), MDI (0.751 g, 3.002 mmol, NCO/OH molar ratio *ca.* 1.10:1), DBTDL (3 drops), and THF (30 mL). **azo-**

**PU4** was obtained as a white fibrous, rubbery solid (2.685 g, 91%).  $M_n(\text{SEC}) = 77,200$  g/mol;  $\bar{D} = 1.70$ .  $^1\text{H NMR}$  (THF- $d_8$ , 400 MHz):  $\delta$  = MDI residue: 8.57 (s, 2H, NH), 8.54 (s, 2H, NH), 7.36 (d, 4H, ArH), 7.03 (d, 4H, ArH), 3.82 (s, 2H, CH<sub>2</sub>-Ar); PTHF residue: 4.09 (t, 4H, CH<sub>2</sub>-OOC), 3.37 (s, 108H, CH<sub>2</sub>-O), 1.69 (s, 4H, CH<sub>2</sub>), 1.58 (s, 108H, CH<sub>2</sub>); BDO residue: 4.12 (d, 4H, CH<sub>2</sub>-O), 1.73 (4H, CH<sub>2</sub> obstructed); **1** residue: 1.33 (s, 12H, CH<sub>3</sub>); end groups: 7.65 (s, 2H, NH<sub>2</sub>), 6.81 (d, 2H, ArH), 6.46 (d, 2H, ArH).

#### ref-PU1 (containing 0 azo motifs per chain)

PTHF (9.994 g, 4.997 mmol), BDO (0.837 g, 9.284 mmol), MDI (3.945 g, 15.765 mmol, NCO/OH molar ratio *ca.* 1.10:1), DBTDL (4 drops), and THF (120 mL). **ref-PU1** was obtained as a white fibrous, rubbery solid (13.298 g, 90%).  $M_n(\text{SEC}) = 119,400$  g/mol;  $\bar{D} = 1.79$ .  $^1\text{H NMR}$  (THF- $d_8$ , 400 MHz):  $\delta$  = MDI residue: 8.57 (s, 2H, NH), 8.54 (s, 2H, NH), 7.36 (d, 4H, ArH), 7.03 (d, 4H, ArH), 3.82 (s, 2H, CH<sub>2</sub>-Ar); PTHF residue: 4.09 (t, 4H, CH<sub>2</sub>-OOC), 3.37 (s, 108H, CH<sub>2</sub>-O), 1.69 (s, 4H, CH<sub>2</sub>), 1.58 (s, 108H, CH<sub>2</sub>); BDO residue: 4.13 (d, 4H, CH<sub>2</sub>-O), 1.73 (4H, CH<sub>2</sub> obstructed); end groups: 6.82 (d, 2H, ArH), 6.47 (d, 2H, ArH), 4.65 (s, 2H, NH<sub>2</sub>).

#### ref-PU2 (containing 0 azo motifs per chain)

PTHF (2.5 g, 1.250 mmol), BDO (0.222 g, 2.469 mmol), MDI (1.036 g, 4.143 mmol, NCO/OH molar ratio *ca.* 1.10:1), DBTDL (3 drops), and THF (30 mL). **ref-PU2** was obtained as a white fibrous, rubbery solid (3.256 g, 88%).  $M_n(\text{SEC}) = 24,000$  g/mol;  $\bar{D} = 1.73$ .  $^1\text{H NMR}$  (THF- $d_8$ , 400 MHz):  $\delta$  = MDI residue: 8.58 (s, 2H, NH), 8.55 (s, 2H, NH), 7.36 (d, 4H, ArH), 7.03 (d, 4H, ArH), 3.82 (s, 2H, CH<sub>2</sub>-Ar); PTHF residue: 4.09 (t, 4H, CH<sub>2</sub>-OOC), 3.36 (s, 108H, CH<sub>2</sub>-O), 1.69 (s, 4H, CH<sub>2</sub>), 1.58 (s, 108H, CH<sub>2</sub>); BDO residue: 4.12 (d, 4H, CH<sub>2</sub>-O), 1.73 (4H, CH<sub>2</sub> obstructed); end groups: 6.81 (d, 2H, ArH), 6.46 (d, 2H, ArH), 4.71 (s, 2H, NH<sub>2</sub>).

## Results and discussion

### Synthesis, characterization and ultrasonic treatment of the polymers

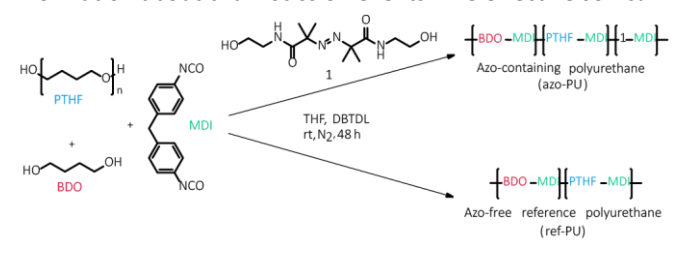
The various polyurethanes used in this study were synthesized by the DBTDL-catalyzed reaction of poly(tetrahydrofuran) (PTHF), 1,4-butanediol (BDO), 4,4'-methylenebis(phenyl isocyanate) (MDI) in the case of **ref-PU**s and additionally the azo-containing diol **1** in the case of the **azo-PU**s, following a procedure that was described previously (Scheme 1).<sup>56</sup> Two **ref-PU**s and four **azo-PU**s with number-average molecular weights ( $M_n$ ) ranging from 24,000 to 119,400 g/mol (ESI, Fig. S1) were made and the average number of azo motifs per polymer chain was varied from 0 to 9.

FT-IR spectra (ESI, Fig. S2) show the expected signals of the urethane carbonyl group at 1730  $\text{cm}^{-1}$ , along with bands at 1530  $\text{cm}^{-1}$  and 1220  $\text{cm}^{-1}$  corresponding to the  $\nu(\text{NH})$  vibration. No band at 2300  $\text{cm}^{-1}$  was observed, indicating that all isocyanate groups had completely reacted.<sup>62</sup>  $^1\text{H NMR}$  spectra show the characteristic peaks of all monomer residues (ESI, Fig. S3-S8) and confirm the expected structures.<sup>56</sup> The methyl protons of the residue of **1** (1.33 ppm) were compared to the methylene protons of the MDI (3.82 ppm) and the amount of azo motif

incorporated into the polymers was thereby shown to match that of the feed.

The main parameters influencing the chain-scission rate, such as ultrasound power density, concentration, vapor pressure, gas solubility, solvent purity, temperature, viscosity and degree of polymerization ( $DP_n$ ) were previously identified.<sup>27,63,64</sup> This study focused specifically on two parameters:  $M_n$  and the content of azo moieties, while literature precedent guided the determination of other experimental parameters. For simplicity,  $M_n$  was chosen as the descriptor for degradation kinetics, but the reader is encouraged to read the reports by May *et al.* and Schaefer *et al.* for a more detailed study on the influence of chain mass vs. length in linear polymers.<sup>27,64</sup>

The sonochemical experiments were carried out under argon in THF at a concentration of 0.75 mg/mL to access kinetic information about chain scission events. The effective sonica-



**Scheme 1.** Synthesis of the azo-containing polyurethanes (azo-PU) and the azo-free reference polymers (ref-PU).

-tion time was set to 90 minutes at a power density of 10.4 W/cm<sup>2</sup>. During sonication, the reaction vessel was placed in an ice bath at 0 °C to ensure that any scission event be the sole consequence of extensional flow and not heating effects. The experiments were monitored by taking aliquots over the course of sonication and by analyzing the molecular weights by SEC (ESI, Fig. S9-S13).

Price *et al.* demonstrated that for poly(styrene) there is a limiting  $M_n$  value, around 30,000 g/mol, below which a polymer cannot undergo ultrasound-induced degradation.<sup>65</sup> Given a polymer with narrow molecular weight distribution, this value is very close to the cutoff molecular weight (the molecular weight below which scission rate is zero). For broad molecular weight distribution, instead, the limiting  $M_n$  might differ substantially from the cutoff molecular weight, because fragments smaller than the cutoff molecular weight can be generated by the sonication process. However, it should be noted that both the limiting  $M_n$  and the cutoff  $M_n$  values strongly depend on the chemical nature of the polymer (*vide infra*). Thus, reference polymers with a “high”  $M_n$  of 119,400 g/mol (**ref-PU1**) and a “low”  $M_n$  of 24,000 g/mol (**ref-PU2**) were made, featuring  $M_n$  values that are four times higher and substantially lower, respectively, than the reported limit (*i.e.*, 30,000 g/mol for poly(styrene)).<sup>65</sup> As anticipated, the two **ref-PU**s displayed rather distinct behavior upon sonication (Fig. 1). The  $M_n$  of **ref-PU1** rapidly decreased to about 55% of the original value, while no change was observed for the low-molecular-weight **ref-PU2**, confirming the existence of a limiting  $M_n$ , below which the polymer chains cannot be cleaved. However, the precise determination of the limiting  $M_n$  for the

polymers studied would require additional experiments with a broader set of polymers having different  $M_n$ , and is beyond the goal of this study.

**Azo-PU1**, with an  $M_n$  of 119,000 g/mol and an average of 9 azo motifs per chain was synthesized to enable a direct comparison with **ref-PU1**. Fig. 2a shows that upon sonication, the SEC traces display an increase in elution time, consistent with a decrease of  $M_n$ . Note that the experimental SEC traces only give apparent molar mass of sonicated polymers and will therefore deviate from the simulated SEC (Fig. 2b, *vide infra*) based on our theoretical model. A comparison of the ratio of the initial number-average molecular weight ( $M_n$ ) and the number-average molecular weight during ultrasonication ( $M_n(t)$ ) solutions of **ref-PU1** and **azo-PU1** (Fig. 1) shows clearly that the latter dissociates considerably faster, and that a lower  $M_n(t)/M_n$  ratio is reached (0.44 vs. 0.55) indicating that the azo motifs, although few in number, influence the degradation kinetics significantly. The possibility to dissociate azo motifs by exposure

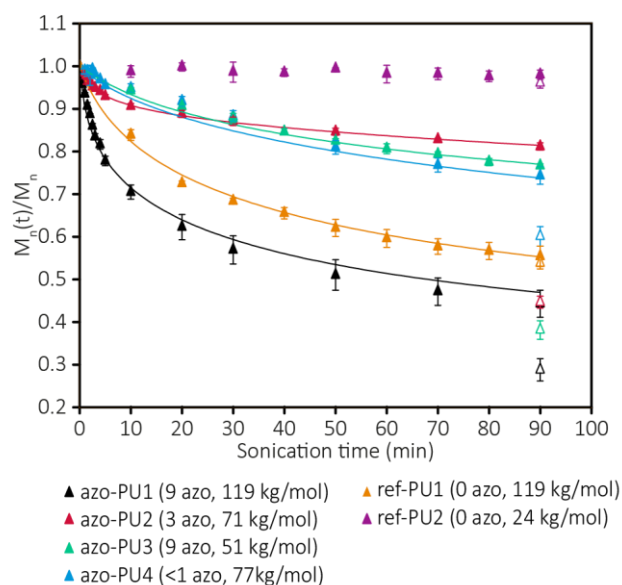


**Fig. 1.** Time-evolution of the ratio of the number-average molecular weight ( $M_n(t)$ ) over the initial number-average molecular weight ( $M_n$ ) for solutions of azo-free and azo-containing polyurethanes upon ultrasonication. The triangles represent the experimentally determined results while the lines are modeled: ref-PU1 (orange) and ref-PU2 (magenta, not modeled), and the azo-containing polyurethanes azo-PU1 (black), azo-PU2 (red), azo-PU3 (green) and azo-PU4 (blue). The open triangles correspond to sonicated samples that were further degraded using UV light (600 mW/cm<sup>2</sup>, 30 s). All experiments were performed in triplicates (0.75 mg/mL in THF, 0 °C, 10.4 W/cm<sup>2</sup>) and results are shown as averages

to ultraviolet light<sup>56</sup> was utilized as a means to elucidate to what extent the azo cleavage was complete after the ultrasonication experiment. Thus, the residual azo moieties were degraded by irradiating previously sonicated polymer solutions with UV light to afford both disproportionated and recombined degradation products. The conditions to achieve complete degradation (320–390 nm, 600 mW/cm<sup>2</sup>, 30 s) have been formerly established, even if some recombination cannot be avoided.<sup>56</sup> SEC measurements were subsequently used to explore the effect of irradiation. Fig. 1 shows that in the case of **azo-PU1** this process

led to a further reduction of the  $M_n(t)/M_n$  ratio from 0.44 to 0.29. As expected, exposure to UV light had a negligible effect on the molecular weight of the reference polymers (Fig. 1). For all polymers, between 39 and 57 % of all azo groups are mechanically cleaved by the sonication process (*vide infra*, see ESI for calculations). In the case of the **azo-PU3** polymer, only 36.5% of the azo moieties are mechanically cleaved. This relation between the quantity of azo groups per chain, chain length and mechanical cleavage of the azo will be further discussed upon introduction of our descriptive model.

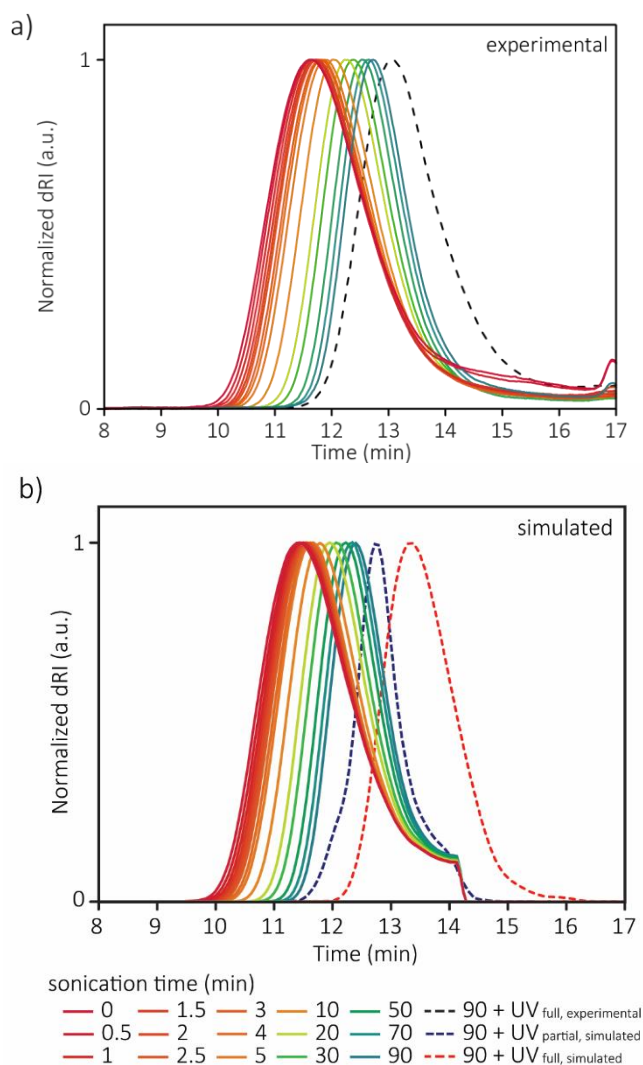


**Fig. 2.** a) Representative SEC traces acquired to monitor the ultrasound-induced degradation of the azo-containing polyurethane **azo-PU1** (0.75 mg/mL in THF, 10.4 mW/cm<sup>2</sup>, 0 °C) followed by a further degradation provoked by exposure to UV light (600 mW/cm<sup>2</sup>, 30 s). b) Simulated SEC traces modeling the ultrasound-induced degradation and the UV-light-triggered decomposition of **azo-PU1**.

### Kinetic modeling

To analyze and describe the kinetics of the ultrasound-induced chain scission in the azo-free and azo-containing polymers discussed, we used a mathematical model based on solving mass balances for polymer chains of all lengths present in the

system, which allows one to follow the time evolution of their respective concentrations. The approach used is similar to that adopted several times in the literature.<sup>52,66-69</sup> If one assumes that chain cleavage only occurs by ultrasound-induced extensional flow, one can suppose that (i) there are two competing processes, namely specific bond cleavage (at the mechanophore) and random bond scission, and (ii) that the former will be kinetically favored (fast) over the latter (slow). We define  $N_n$  as the number concentration of polymer chains with mass  $n$ . The longest chain has a mass  $N$  such that the number concentration of polymer chains with highest molecular weight is  $N_N$ . The mass balance of these chains can be expressed as:

$$\frac{dN_N}{dt} = -\left(K_{S,N}(t) + K_{F,N}(t)\right) \cdot N_N \quad (1)$$

since the chains of mass  $N$  can only be broken by ultrasonication. In Equation (1),  $K_{S,N}$  and  $K_{F,N}$  are the two kinetic constants, describing the slow unspecific and the fast specific bond cleavage processes, respectively. Note that both constants are time-dependent. The mass balance of shorter chains, which can be generated from parent chains and also undergo scission is:

$$\frac{dN_n}{dt} = -\left(K_{S,n}(t) + K_{F,n}(t)\right) \cdot N_n + \sum_{i=m}^l \left(K_{S,i}(t) + K_{F,i}(t)\right) \cdot N_i \cdot \Gamma_{i,n} \quad (2)$$

where the indices  $m$  and  $l$  correspond to the shortest and longest chains that can produce fragments of mass  $n$ .  $\Gamma_{i,n}$  is the fragment distribution function, *i.e.*, the probability that scission of a chain with mass  $i$  will produce a fragment with mass  $n$  (where  $n < i$ ). Finally, the mass balance of chains that can only be produced by a scission event, but cannot be broken by the sonication process is:

$$\frac{dN_n}{dt} = \sum_{i=m}^l \left(K_{S,i}(t) + K_{F,i}(t)\right) \cdot N_i \cdot \Gamma_{i,n} \quad (3)$$

The kinetic constants are a function of the chain length and of time, and can be expressed by:

$$K_{S,i}(t) = \kappa_S (i - c_{off})^2 (1 - p(t))$$

$$K_{F,i}(t) = \kappa_F [(i - c_{off})]^2 p(t) \quad (4)$$

In Equation (4),  $c_{off}$  is the cutoff mass below which no scission occurs. It might be fair to assume that  $c_{off}$  for a polymer chain depends on the strength of the bond to be broken. We attempted to use a smaller  $c_{off}$  for the scission of azo bonds, but the difference was negligible for long polymers. Therefore, for the sake of reducing the number of arbitrary parameters in the model, we decided to keep the cutoff molecular weight equal for both processes.  $\kappa_S$  and  $\kappa_F$  are two constants, which are adjusted to fit the experimental data. It is worth noting that sonication scission rates are a function of polymer concentration. Therefore, different polymer concentrations will correspond to different scission rate constants. Additionally, the constants might also be a function of the polymeric composition (molecular weight distribution). Finally,  $p(t)$  represents the fraction of azo moieties in the polymer chain. It is assumed that the fraction of azo moieties decreases in time,

while remaining identical for all polymer chains, independent of their lengths. However, since the *fraction* of azo moieties is identical for all chains, their *absolute number* in a given polymer chain is proportional to the chain molecular weight. The dependence of the chains scission rate constants on molecular weight in Equation (4) is consistent with the physical model proposed by Martijn *et al.*,<sup>66</sup> which predicts that the force required to break a polymer chain, via implosion of a bubble, scales with the square of the chain molecular weight. Similarly, the associated scission rate constant also scales proportionally for the same reasoning.

The fragment distribution function  $\Gamma_{i,n}$  obeys the following constraint:

$$\sum_1^{i-1} n \cdot \Gamma_{i,n} = i \quad (5)$$

expressing mass conservation upon scission, *i.e.*, the sum of the masses of all fragments equals the mass of the original chain.

As previously mentioned, most recent reports in the field have concluded that the mechanical chain cleavage is a process that fundamentally occurs near the center of the polymer chains. These observations have been achieved using polymers with chain-centered mechanophores to procure a narrower distribution of products.<sup>63</sup> Furthermore, it was observed that the mechanical forces acting gave rise to cleavage approximately near the central 15% of a polymer chain.<sup>70</sup> The assumption for the breakage process here is that the fragment distribution function is assumed to be a Gaussian, centered at the center of each chain, and rapidly decaying:

$$\Gamma_{i,n} = A e^{-\frac{(\frac{i}{2}-n)^2}{2(\sigma^2)}} \quad (6)$$

In Equation (6),  $\sigma$  is the parameter determining the variance of the Gaussian distribution, *i.e.*, its broadness. In this work, this value has been fixed to 0.15. The normalization constant  $A$  is directly determined from Equation (5).

Additionally, the mass balance of the azo groups must be considered. Such equation is given as a balance over the average fraction of azo-groups in the chains, assumed to be the same for all chains independently of the molecular weight of the chain:

$$\frac{d(p(t) \sum_{n=1}^N (n-1) \cdot N_n)}{dt} = - \sum_{n=1}^N n \cdot K_{F,n}(t) \cdot N_n \quad (7)$$

The term in the first bracket is  $p(t)$  times the total number of bonds in the polymer chains. Equation (7) can be re-written as:

$$\frac{dp(t)}{dt} = - \frac{\sum_{n=1}^N (n-1) \cdot K_{F,n}(t) \cdot N_n}{\sum_{n=1}^N (n-1) \cdot N_n} - \frac{\sum_{n=1}^N (n-1) \cdot \frac{dN_n}{dt}}{\sum_{n=1}^N (n-1) \cdot N_n} \quad (8)$$

As an initial condition, we have used the molecular weight distribution of the polymer before sonication, obtained from SEC data. The azo moieties have been uniformly distributed inside the polymer chains, proportionally to their molecular weight. For example, for **azo-PU1**, a chain with a molecular weight of 120 kg/mol has 9 azo groups per chain. Since the molecular weight distribution of this polymer is quite broad, there are polymer chains with a molecular weight of  $1.2 \cdot 10^3$  kg/mol, which have 90 azo units, and chains with a molecular

weight of 26 kg/mol, which contain only two azo group per chain. The solution for the system of non-linear differential equations must be obtained numerically. A pivot-based approach, as developed by Kumar and Ramkrishna,<sup>71</sup> has been used for this purpose, with 200 pivots used in all simulations. The time evolution of the number average molecular weight,  $M_n$  can be obtained by summing over all kinetic equations:

$$\frac{dM_n}{dt} = \frac{d}{dt} \left( \frac{\sum_i N_i M_i}{\sum_i N_i} \right) = - \frac{\sum_i N_i M_i}{(\sum_i N_i)^2} \sum_i \frac{dN_i}{dt} \quad (9)$$

This can be rewritten as:

$$\frac{dM_n}{dt} = - \frac{\sum_i N_i M_i}{(\sum_i N_i)^2} \sum_i \left( - (K_{S,n}(t) + K_{F,n}(t)) \cdot N_n + \sum_{i=m}^l (K_{S,i}(t) + K_{F,i}(t)) \cdot N_i \cdot \Gamma_{i,n} \right) \quad (10)$$

The last equation can be reformulated as follows:

$$\begin{aligned} \frac{dM_n}{dt} &= - \frac{M_n}{\sum_i N_i} \sum_i \left( - (K_{S,i}(t) + K_{F,i}(t)) \cdot N_i + \sum_j^l (K_{S,j}(t) + K_{F,j}(t)) \cdot N_j \cdot \Gamma_{j,i} \right) \\ &= - (k_1(t)(1-p(t)) + k_2(t)p(t)) \cdot M_n \end{aligned} \quad (11)$$

In Equation (11),  $k_2(t)$  and  $k_1(t)$  are effective average kinetic constants, which are both functions of time. The time dependence of these constants is due to their dependence on the molecular weight distribution  $N_j(t)$ , which is a function of time. Both constants rapidly change with time, especially at the beginning of the sonication process. Particularly, the initial polymer molecular weight is high, thus the corresponding initial scission rate is thus also high. Their explicit expressions are:

$$\begin{aligned} k_2(t) &= \frac{\sum_i (K_{S,i} \cdot N_i + \sum_j K_{S,j} \cdot N_j \cdot \Gamma_{j,i})}{(\sum_i N_i)} \\ k_1(t) &= \frac{\sum_i (\kappa_F [i - c_{off}]^2 \cdot N_i + \sum_j \kappa_F [j - c_{off}]^2 \cdot N_j \cdot \Gamma_{j,i})}{(\sum_i N_i)} \end{aligned} \quad (12)$$

As can be seen from Fig. 3, the rate constant associated with the scission of the azo groups is considerably higher than the rate constant associated with unspecific chain cleavage and both constants decrease over time. Although  $k_2(t) \gg k_1(t)$ , the overall chain scission rate also depends on the fraction of the respective cleavable groups in the polymer  $p(t)$ , which is much lower for the azo groups.

From this model, it is possible to derive a general equation describing the time evolution of the molecular weight, *i.e.*, Equation (11). Such an equation shows that  $M_n(t)$  is described by a modified first-order kinetic equation, with two effective kinetic constants that are a function of time. This means that  $M_n(t)$  cannot simply be described by a single exponential function, as the kinetic constants are a function of time. The same approach can also be utilized to describe the time evolution of polymer chains not containing azo moieties, by simply setting  $\kappa_F$  equal to zero. Fig. 1 shows the decay of the normalized molecular weight vs time of the different azo-containing polymers, which are in excellent agreement with the proposed model. These curves have been obtained by adjusting two parameters in the model,  $\kappa_S$  and  $\kappa_F$  in Equation (4), to fit

the experimentally determined number-average molecular weight. The full molecular weight distribution time evolution has also been fitted. From this curve fit, information about the evolution of polymer chain populations in the system, including the number-average molecular weight, can then be readily extracted by using Equation (11). The molecular weight evolution of reference polymers without azo mechanophores, shown in Fig. 1, can also be described with this model in which only one rate constant was used (and therefore only one parameter,  $\kappa_S$ , was adjusted). It is important to highlight that the same values of parameters  $\kappa_S$  and  $\kappa_F$  have been used in all simulations. The  $\kappa_S = 7 \cdot 10^{-12} \text{ s}^{-1}$  value was obtained from fitting the data of **ref-PU1**, while the  $\kappa_F = 8 \cdot 10^{-9} \text{ s}^{-1}$  value was obtained from cleavage data of the azo-containing polymers. The fact that the same values have been used for all polymers is an indication of the robustness of the modeling approach used in this work.

In order to provide a better understanding of the order of magnitude of the two effective rate constants,  $k_1(t)$  and  $k_2(t)$ , their mean average values over the entire sonication time, hereby referred to as  $k_{1,\text{eff}}$  and  $k_{2,\text{eff}}$ , are reported in Table 1. For example,  $M_n(t)$  of the high molecular weight **ref-PU1** was fitted with the model, affording a mean value of the effective constant  $k_{2,\text{eff}}$  of  $0.0002 \text{ min}^{-1}$ . It is worth noting that these constants are

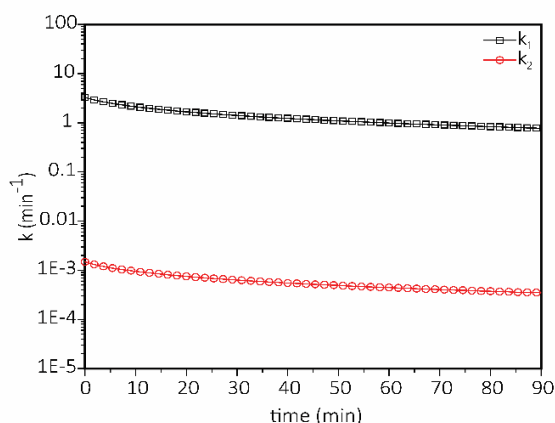


**Fig. 3.** Effective scission rate constants for the azo-containing polyurethane **azo-PU1** polymer as a function of time. These curves were plotted by fitting the data with two parameters in the model,  $\kappa_S$  and  $\kappa_F$  in Equation (1).

average values, which depend on the entire molecular weight distribution. Fig. S18-S21 show the full-time evolution of the effective kinetic constants used to describe the time evolution of the number-average molecular weight of all polymers. The supplementary Figs. illustrate that both rate constants decay as a function of time because of the progressive decrease in the polymer molecular weight. Both constants, despite being at different orders of magnitude, decay at roughly the same rate. While the values of the constants obtained from the simulations vary slightly from sample to sample, they provide a clear trend: random bond scission dominates during the end-phase of the sonication, whereas mechanophore cleavage is very rapid and dominates the initial sonication phase. Thus,  $k_{1,\text{eff}}$  is generally three orders of magnitude larger than  $k_{2,\text{eff}}$  (Table 1), which is reflected by the three orders of magnitude difference in the

parameter values  $\kappa_S$  and  $\kappa_F$ . These values already take into account the smaller number of azo units in the chains. The  $k_{2,\text{eff}}$  values calculated for the **ref-PU**s and the **azo-PU**s were slightly different but of the same order of magnitude, because of the different molecular weight

**Table 1.** Description, modeling parameters, and effective cleavage rate constants of the sonicated azo-containing polyurethanes **azo-PU**s and the azo-free reference polymers **ref-PU**s.

Polymer	$M_n^{[a]}$ (g/mol)	Azo nbr <sup>[b]</sup>	Cleavage rate constants <sup>[c]</sup> ( $\text{min}^{-1}$ )		Fraction of azo-groups after sonication <sup>[d]</sup>
			$k_{1,\text{eff}}$	$k_{2,\text{eff}}$	
azo-PU1	119,000	9	1.3495	0.0006	0.7198
azo-PU2	70,900	3	0.5520	0.00025	0.8898
azo-PU3	51,300	9	0.2882	0.00009	0.8301
azo-PU4	77,200	<1	0.6764	0.0003	0.9504
ref-PU1	119,400	0	-	0.0002	-
ref-PU2	24,000	0	-	-	-

[a] Determined by size exclusion chromatography (SEC). [b] Average number of azo motifs per chain molecule determined from the measured  $M_n$  and the composition of the reaction feed, assuming quantitative incorporation.<sup>56</sup> [c] Obtained by modeling the  $M_n$  decrease as reflected by SEC data after sonication experiments (0.75 mg/mL in THF, 10.4 W/cm<sup>2</sup>, 0 °C).<sup>56</sup> [d] Calculated by modeling and reported in Fig. 4.

distribution of the two polymers. The model provides very good agreement with the experimental data for **ref-PU**s as well as **azo-PU**s, supporting the proposed kinetic hypothesis. In order to further show the model prediction ability, Fig. S14-S17 show the simulated SEC curves for all polymers. Due to the discrete nature of the pivot-based method used to solve the kinetics equations, the simulated SEC curves, can have rough profiles in the low molecular weight region. Therefore, a numerical smoothing procedure has been applied and discussed in Fig. S14-S17. It is possible to observe that the model can predict quite well the time evolution of the molecular weight distribution of the polymers, thus confirming the reliability of the approach utilized.

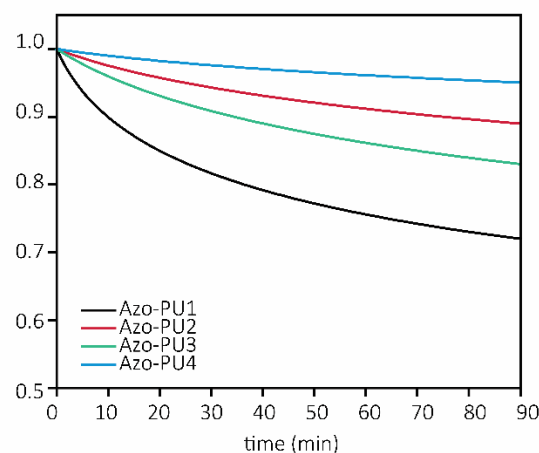


**Fig. 4.** Simulated decrease of the azo moieties content as a function of the ultrasonication time for the azo-containing polyurethanes **azo-PU1** (black line), **azo-PU2** (red line), **azo-PU3** (green line), and **azo-PU4** (blue line).

### Scission behavior as a function of chain length and azo motifs

The present section aims to describe the relationship between the azo content and the chain length. As demonstrated above, the azo motif is a powerful tool to understand the details of specific chain scission. The potential to further cleave the azo groups that were still intact upon sonication using post-treatment UV irradiation should enable one to compare the scission kinetics. The azo-containing polyurethane **azo-PU1** (9 azo motifs per chain and a  $M_n$  of 119,000 g/mol) exhibited a selective bond scission as a result of its high molecular weight (*vide supra*) and the relatively high azo content. Simulations indicate that this reduction of the number of azo groups coincides with the remaining 72% of the azo moieties that survived the sonication process (Fig. 4).

The stark difference between the two rate constants explain the preferential scission of the azo groups and the results for all other azo-containing polymers. Despite a four order of magnitude greater effective rate constant for azo cleavage, the simulation results also indicate that the fraction of azo moieties cleaved is only 28% for **azo-PU1**. It drops to less than 12% for **azo-PU2**, assumedly due to the lower molecular weight and lower azo fraction. This percentage further decreases to 17% in the case of **azo-PU3**, and about 5% in the case of **azo-PU4**. Despite the large fraction of azo moieties per chain in **azo-PU3** (equal to that of **azo-PU1**), the lower molecular weight led to fewer scission events. Accordingly, this result demonstrates that the molecular weight of **azo-PU3** is near the limiting value for a mechanically induced degradation.

The high-molecular-weight azo-free reference polyurethane **ref-PU1** exhibited solely random bond scission events. Compared to **azo-PU1**, the absence of azo moieties led to a slower and less pronounced molecular weight decrease (Fig. 1), in spite of their similar molecular weight. In particular, the decrease in molecular weight is lower at the very beginning of the sonication process, where in the case of **azo-PU1** polymer the azo moieties are primarily cleaved. At later sonication times, the rates of molecular weight decay are similar for both cases as the final molecular weight approaches the cutoff. The calculated time decay of the fraction of azo moieties for all azo-containing polymers is reported in the ESI, in Fig. 4.

Finally, UV light irradiation was performed after sonication to cleave some of the residual azo moieties and thus elucidate the extent of the mechanically driven cleavage. Indeed, as already described in a previous study,<sup>56</sup> azo motifs that are part of a polymer backbone can be rapidly degraded upon exposure to ultraviolet light. This characteristic was employed here to selectively cleave the remaining azo motifs that had not been affected by the ultrasound-triggered cleavage. UV irradiation demonstrated that the scission events did not cleave all the azo moieties (*i.e.*, when the  $M_n$  limit was achieved), and also proved that thermally induced cleavage can be excluded. As expected, the azo-free reference polymers did not show any further  $M_n$  decrease following the UV light irradiation. We extended our modeling approach to estimate the molecular weight distribution of polymer chains after UV irradiation, assuming complete cleavage of all azo moieties. The mathematical details

of the procedure followed are presented in the ESI. Under the assumption that the remaining azo groups are randomly distributed in the polymer chains, Fig. 2b, and S14-S16 show the simulated SEC curves after sonication. In all cases, the predicted molecular weight distributions are much lower than the experimental ones. This implies that UV irradiation is also not able to cleave all the azo moieties remaining after sonication or that some radical recombination occurs. A simple calculation shows this. If one assumes that the azo moieties are evenly spaced inside a polymer chain, by considering, for example, the **azo-PU1** polymer (9 azo groups per chain) the scission of all the azo moieties would lead to a decrease in the number average molecular weight by a factor of 10. A more precise calculation, assuming the azo moieties are randomly distributed inside a chain, shows that a decrease in the number average molecular weight by a factor 8 should be expected. On the other hand, SEC data indicate that the average molecular weight of the polymer after sonication and UV irradiation is only 30% of the initial value. We then used the random distribution model to estimate that, after sonication and UV irradiation, only about 39% of the azo groups have been cleaved in the **azo-PU1** polymer (see Fig. S22 for potential products). For the other polymers, the percentage of azo moieties cleaved after sonication and UV irradiation, estimated with the same strategy, is 33% for **azo-PU2**, 23% for **azo-PU3** and 57% for **azo-PU4**. The correspondingly predicted molecular weight distributions are shown in the supporting information.

### Conclusions

In summary, a new kinetic mechanism has been reported for chains containing multiple, randomly distributed scissile mechanophores. This model was verified with polyurethanes containing multiple azo mechanophores randomly distributed within the polymer chains.  $M_n$  as a function of the sonication time exhibited an exponential decay for the polymers with high molecular weight. Based on ultrasonication experiments, a detailed model capable of predicting the time evolution of entire molecular weight distribution of a polymer undergoing sonication has been developed and used to estimate the effective rate constants of the azo-containing polymers, corresponding to two competitive events, *i.e.*, the mechanophore cleavage ( $k_{1,eff}$ ) and the random bond scission ( $k_{2,eff}$ ). By fitting the experimental data with the model, it has been found that the first event is clearly favored compared to the second one (1000 faster). Additionally, this strategy demonstrated, besides the content of mechanophores per chain, the important role of the molecular weight on the ultrasonic rate cleavage of mechanoresponsive polyurethanes. All analytical data supported the existence of limiting  $M_n$ , even though not precisely determined herein. This work describes an understanding about the behavior of mechanophores randomly incorporated into polyurethanes. One of the strengths of the present model is the ability to predict the molecular weight (and molecular weight distributions) even after irradiation of the polymer chains by UV light. It is shown that UV irradiation cleaves some of the azo moieties, but not all of them, and the

model can make a prediction of the number of azo moieties remaining in the polymer after irradiation. While this paper answers an important question regarding the ultrasonic cleavage of scissile mechanophores distributed along polymeric chains, many other fundamental questions regarding degradation remain unanswered in part due to the convoluted nature of the ultrasonication process, which makes this area of polymer science particularly attractive.

### Conflicts of interest

There are no conflicts to declare.

### Acknowledgements

The research leading to these results has received funding from the European Research Council under the European Union's Seventh Framework Programme (FP7/2007-2013)/ERC grant agreement n° 291490-MERESPO. This work was supported also by the Swiss National Science Foundation (Grant PP00P2133597/1), American Chemical Society Petroleum Research Fund (ACS PRF) grant #57957, National Center of Competence in Research for Bio-Inspired Materials, and the Adolphe Merkle Foundation. C. H. L. acknowledges support from the National Science Foundation Research Trainee (NSF NRT) Program Award #1449999. The authors would like to thank Dr. Dafni Moatsou, Dr. Laura Rodríguez-Lorenzo and Dr. Janak Sapkota for useful discussions.

### Notes and references

- J. Li, C. Nagamani and J. S. Moore, *Accounts of Chemical Research*, 2015, **48**, 2181-2190.
- K. Imato, T. Kanehara, T. Ohishi, M. Nishihara, H. Yajima, M. Ito, A. Takahara and H. Otsuka, *Acs Macro Lett*, 2015, **4**, 1307-1311.
- Z. J. Wang, Z. Y. Ma, Y. Wang, Z. J. Xu, Y. Y. Luo, Y. Wei and X. R. Jia, *Adv. Mater.*, 2015, **27**, 6469-6474.
- C. P. Kabb, C. S. O'Bryan, C. D. Morley, T. E. Angelini and B. S. Sumerlin, *Chem Sci*, 2019, **10**, 7702-7708.
- G. R. Gossweiler, C. L. Brown, G. B. Hewage, E. Sapiro-Gheiler, W. J. Trautman, G. W. Welshofer and S. L. Craig, *ACS Appl. Mater. Interfaces*, 2015, **7**, 22431-22435.
- C. E. Diesendruck, B. D. Steinberg, N. Sugai, M. N. Silberstein, N. R. Sottos, S. R. White, P. V. Braun and J. S. Moore, *J. Am. Chem. Soc.*, 2012, **134**, 12446-12449.
- Y. Lin, T. B. Kouznetsova and S. L. Craig, *J Am Chem Soc*, 2020, **142**, 99-103.
- J. M. Clough, A. Balan, T. J. van Daal and R. P. Sijbesma, *Angew. Chem. Int. Ed.*, 2016, **55**, 1445-1449.
- X. Hu, T. Zeng, C. C. Husic and M. J. Robb, *J. Am. Chem. Soc.*, 2019, **141**, 15018-15023.
- M. B. Larsen and A. J. Boydston, *J. Am. Chem. Soc.*, 2014, **136**, 1276-1279.
- Z. Li, R. Toivola, F. Ding, J. Yang, P.-N. Lai, T. Howie, G. Georgeson, S.-H. Jang, X. Li, B. D. Flinn and A. K. Y. Jen, *Adv. Mater.*, 2016, **28**, 6592-6597.
- G. A. Filonenko, D. P. Sun, M. Weber, C. Muller and E. A. Pidko, *Journal of the American Chemical Society*, 2019, **141**, 9687-9692.
- A. L. B. Ramirez, Z. S. Kean, J. A. Orlicki, M. Champhekar, S. M. Elsagr, W. E. Krause and S. L. Craig, *Nat Chem*, 2013, **5**, 757-761.
- R. T. M. Jakobs, S. Ma and R. P. Sijbesma, *Acs Macro Lett*, 2013, **2**, 613-616.
- D. W. R. Balkenende, S. Coulibaly, S. Balog, Y. C. Simon, G. L. Fiore and C. Weder, *J. Am. Chem. Soc.*, 2014, **136**, 10493-10498.
- Z. Shi, J. Wu, Q. Song, R. Gostl and A. Herrmann, *J Am Chem Soc*, 2020, **142**, 14725-14732.
- A. R. Sulkanen, J. Sung, M. J. Robb, J. S. Moore, N. R. Sottos and G. Y. Liu, *J Am Chem Soc*, 2019, **141**, 4080-4085.
- C. P. Kabb, R. N. Carmean and B. S. Sumerlin, *Chemical Science*, 2015, **6**, 5662-5669.
- A. Levy, R. Feinstein and C. E. Diesendruck, *Journal of the American Chemical Society*, 2019, **141**, 7256-7260.
- M. Zhang and G. De Bo, *J Am Chem Soc*, 2019, **141**, 15879-15883.
- M. Zhang and G. De Bo, *J Am Chem Soc*, 2018, **140**, 12724-12727.
- M. Zhang and G. De Bo, *J Am Chem Soc*, 2020, **142**, 5029-5033.
- B. Lee, Z. Niu and S. L. Craig, *Angew Chem Int Ed Engl*, 2016, **55**, 13086-13089.
- Y. J. Lin, Y. D. Zhang, Z. Wang and S. L. Craig, *Journal of the American Chemical Society*, 2019, **141**, 10943-10947.
- L. J. Wang, X. J. Zhou, X. H. Zhang and B. Y. Du, *Macromolecules*, 2016, **49**, 98-104.
- M. M. Caruso, D. A. Davis, Q. Shen, S. A. Odom, N. R. Sottos, S. R. White and J. S. Moore, *Chem Rev*, 2009, **109**, 5755-5798.
- P. A. May, N. F. Munaretto, M. B. Hamoy, M. J. Robb and J. S. Moore, *Acs Macro Lett*, 2016, **5**, 177-180.
- S. L. Potisek, *J. Am. Chem. Soc.*, 2007, **129**, 13808-13809.
- S. Karthikeyan, S. L. Potisek, A. Piermattei and R. P. Sijbesma, *J. Am. Chem. Soc.*, 2008, **130**, 14968-14969.
- M. J. Kryger, A. M. Munaretto and J. S. Moore, *J. Am. Chem. Soc.*, 2011, **133**, 18992-18998.
- Z. S. Kean, A. L. Black Ramirez, Y. Yan and S. L. Craig, *J. Am. Chem. Soc.*, 2012, **134**, 12939-12942.
- T. Shiraki, C. E. Diesendruck and J. S. Moore, *Faraday Discuss.*, 2014, **170**, 385-394.
- M. J. Robb and J. S. Moore, *J. Am. Chem. Soc.*, 2015, **137**, 10946-10949.
- H.-Y. Duan, Y.-X. Wang, L.-J. Wang, Y.-Q. Min, X.-H. Zhang and B.-Y. Du, *Macromolecules*, 2017, **50**, 1353-1361.
- Z. S. Kean, G. R. Gossweiler, T. B. Kouznetsova, G. B. Hewage and S. L. Craig, *Chem Commun (Camb)*, 2015, **51**, 9157-9160.
- R. Stevenson and G. De Bo, *J Am Chem Soc*, 2017, **139**, 16768-16771.
- I. M. Klein, C. C. Husic, D. P. Kovacs, N. J. Choquette and M. J. Robb, *J Am Chem Soc*, 2020, DOI: 10.1021/jacs.0c06868.
- K. L. Berkowski, S. L. Potisek, C. R. Hickenboth and J. S. Moore, *Macromolecules*, 2005, **38**, 8975-8978.
- M. V. Encina, E. Lissi, M. Sarasúa, L. Gargallo and D. Radic, *Journal of Polymer Science: Polymer Letters Edition*, 1980, **18**, 757-760.
- S. J. Kim and D. H. Reneker, *Polym. Bull.*, 1993, **31**, 367-374.

41. J. M. J. Paulusse and R. P. Sijbesma, *Angew. Chem. Int. Ed.*, 2004, **43**, 4460-4462.
42. C. K. Lee, D. A. Davis, S. R. White, J. S. Moore, N. R. Sottos and P. V. Braun, *J. Am. Chem. Soc.*, 2010, **132**, 16107-16111.
43. B. Lee, Z. Niu, J. Wang, C. Slebodnick and S. L. Craig, *J. Am. Chem. Soc.*, 2015, **137**, 10826-10832.
44. B. H. Bowser and S. L. Craig, *Polymer Chemistry*, 2018, **9**, 3583-3593.
45. J. M. Lenhardt, A. L. Black and S. L. Craig, *J. Am. Chem. Soc.*, 2009, **131**, 10818-10819.
46. J. M. Lenhardt, M. T. Ong, R. Choe, C. R. Evenhuis, T. J. Martinez and S. L. Craig, *Science*, 2010, **329**, 1057-1060.
47. H. M. Klukovich, Z. S. Kean, S. T. Iacono and S. L. Craig, *J. Am. Chem. Soc.*, 2011, **133**, 17882-17888.
48. H. M. Klukovich, Z. S. Kean, A. L. B. Ramirez, J. M. Lenhardt, J. Lin, X. Hu and S. L. Craig, *J. Am. Chem. Soc.*, 2012, **134**, 9577-9580.
49. Z. S. Kean, Z. Niu, G. B. Hewage, A. L. Rheingold and S. L. Craig, *J. Am. Chem. Soc.*, 2013, **135**, 13598-13604.
50. R. Stevenson, M. Zhang and G. De Bo, *Polymer Chemistry*, 2020, **11**, 2864-2868.
51. B. Lee, Z. Niu, J. Wang, C. Slebodnick and S. L. Craig, *J Am Chem Soc*, 2015, **137**, 10826-10832.
52. M. Di Giannantonio, M. A. Ayer, E. Verde-Sesto, M. Lattuada, C. Weder and K. M. Fromm, *Angew Chem Int Ed Engl*, 2018, **57**, 11445-11450.
53. Y. Sha, Y. Zhang, E. Xu, C. W. McAlister, T. Zhu, S. L. Craig and C. Tang, *Chem Sci*, 2019, **10**, 4959-4965.
54. Z. S. Kean, A. L. B. Ramirez and S. L. Craig, *J Polym Sci Pol Chem*, 2012, **50**, 3481-3484.
55. Y. Sha, Y. Zhang, E. Xu, Z. Wang, T. Zhu, S. L. Craig and C. Tang, *ACS Macro Lett*, 2018, **7**, 1174-1179.
56. M. A. Ayer, Y. C. Simon and C. Weder, *Macromolecules*, 2016, **49**, 2917-2927.
57. M. A. Ayer, S. Schrettl, S. Balog, Y. C. Simon and C. Weder, *Soft Matter*, 2017, **13**, 4017-4023.
58. Y. Q. Dai, H. Sun, S. Pal, Y. L. Zhang, S. Park, C. P. Kabb, W. D. Wei and B. S. Sumerlin, *Chemical Science*, 2017, **8**, 1815-1821.
59. H. Sun, D. J. Dobbins, Y. Q. Dai, C. P. Kabb, S. J. Wu, J. A. Alfurhood, C. Rinaldi and B. S. Sumerlin, *Acs Macro Letters*, 2016, **5**, 688-693.
60. B. Lee, Z. B. Niu, J. P. Wang, C. Slebodnick and S. L. Craig, *Journal of the American Chemical Society*, 2015, **137**, 10826-10832.
61. H. Mutlu, C. M. Geiselhart and C. Barner-Kowollik, *Mater Horiz*, 2018, **5**, 162-183.
62. Z. Y. Ren, H. P. Wu, J. M. Ma and D. Z. Ma, *Chin. J. Polym. Sci.*, 2004, **22**, 225-230.
63. P. A. May and J. S. Moore, *Chem. Soc. Rev.*, 2013, **42**, 7497-7506.
64. M. Schaefer, B. Icli, C. Weder, M. Lattuada, A. F. M. Kilbinger and Y. C. Simon, *Macromolecules*, 2016, **49**, 1630-1636.
65. G. J. Price and P. F. Smith, *Polymer*, 1993, **34**, 4111-4117.
66. M. W. A. Kuijpers, P. D. Iedema, M. F. Kemmere and J. T. F. Keurentjes, *Polymer*, 2004, **45**, 6461-6467.
67. A. Tayal, R. M. Kelly and S. A. Khan, *Macromolecules*, 1999, **32**, 294-300.
68. G. J. Heymach and D. E. Jost, *Journal of Polymer Science Part C: Polymer Symposia*, 1968, **25**, 145-153.
69. M. Tanigawa, M. Suzuto, K. Fukudome and K. Yamaoka, *Macromolecules*, 1996, **29**, 7418-7425.
70. K. S. Suslick and G. J. Price, *Annu Rev Mater Sci*, 1999, **29**, 295-326.
71. S. Kumar and D. Ramkrishna, *Chem. Eng. Sci.*, 1996, **51**, 1311-1332.